

# Structure of PAK1 in an Autoinhibited Conformation Reveals a Multistage Activation Switch

Ming Lei,\* Wange Lu,\* Wuyi Meng,†  
Maria-Carla Parrini,\* Michael J. Eck,†  
Bruce J. Mayer,\* Stephen C. Harrison\*†§

\*Laboratory of Molecular Medicine and

†Howard Hughes Medical Institute

Children's Hospital

320 Longwood Avenue

Boston, Massachusetts 02115

†Department of Cancer Biology

Dana-Farber Cancer Institute

Boston, Massachusetts 02115

## Summary

The p21-activated kinases (PAKs), stimulated by binding with GTP-liganded forms of Cdc42 or Rac, modulate cytoskeletal actin assembly and activate MAP-kinase pathways. The 2.3 Å resolution crystal structure of a complex between the N-terminal autoregulatory fragment and the C-terminal kinase domain of PAK1 shows that GTPase binding will trigger a series of conformational changes, beginning with disruption of a PAK1 dimer and ending with rearrangement of the kinase active site into a catalytically competent state. An inhibitory switch (IS) domain, which overlaps the GTPase binding region of PAK1, positions a polypeptide segment across the kinase cleft. GTPase binding will refold part of the IS domain and unfold the rest. A related switch has been seen in the Wiskott-Aldrich syndrome protein (WASP).

## Introduction

The p21-activated kinases (PAKs) are members of a family of serine/threonine protein kinases defined by their interaction with the small GTPases, Cdc42 and Rac (Manser et al., 1994; Daniels and Bokoch, 1999). There are four known family members (PAK1–4) in mammals; Ste20 and Cla4 are budding yeast homologs (Lim et al., 1996; Sells and Chernoff, 1997; Knaus and Bokoch, 1998). The GTP-bound forms of Cdc42 and Rac regulate assembly of the actin cytoskeleton, in part by stimulation of PAKs and in part by activation of the intermediate switch proteins, WASP (Wiskott-Aldrich syndrome protein) and N-WASP (Rohatgi et al., 1999; Sells et al., 1999). One way in which PAKs can influence actin organization and cell polarity is through phosphorylation of substrates such as myosin light-chain kinase and myosin itself (Brzeska et al., 1997; Buss et al., 1998; Sanders et al., 1999). PAKs can respond to receptor-mediated signals that direct their recruitment to the plasma membrane and subsequent activation (Bokoch et al., 1996; Galisteo et al., 1996; Lu et al., 1997; Bubeck-Wardenburg et al., 1998; Yablonski et al., 1998; Lu and Mayer, 1999).

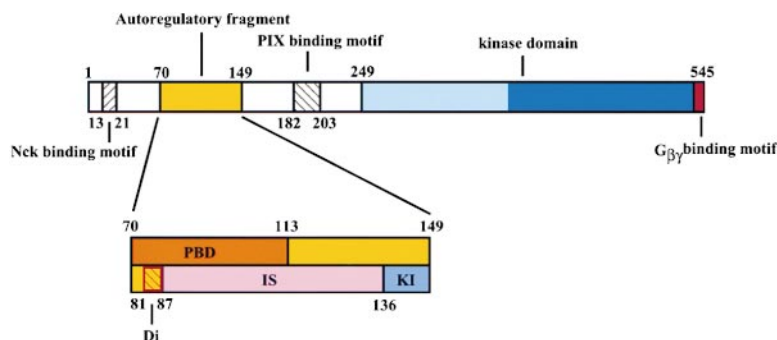
This recruitment is thought to be critical for axon guidance and targeting in *Drosophila*, probably through regulation of the actin cytoskeleton at the growth cone of migrating neurons (Hing et al., 1999). PAKs also activate MAP kinase cascades in vertebrates and in yeast (Bagrodia et al., 1995; Zhang et al., 1995; Brown et al., 1996; Frost et al., 1996). In cells infected with HIV-1, PAKs bind the HIV Nef protein and may have a role in HIV pathogenesis (Cullen, 1996; Renkema et al., 1999; Fackler et al., 2000).

PAKs 1–3 have an N-terminal half that includes autoregulatory and interaction segments and a C-terminal kinase domain. Figure 1 shows the organization of functional regions within the PAK1 polypeptide chain. The sequences required for tight binding to Cdc42 and Rac have been studied by analyzing properties of truncated fragments and site-directed mutants (Burbelo et al., 1995; Rudolph et al., 1998; Thompson et al., 1998; Zhao et al., 1998; Tu and Wigler, 1999), and by determining the solution structure of a complex of Cdc42 with the homologous segment of WASP (Abdul-Manan et al., 1999). The GTPase binding region has acquired various designations: we use "PBD" (p21 binding domain) in this paper. Overlapping but not coincident with the PBD of PAK1–3 is a segment implicated in autoinhibition (Frost et al., 1998; Zhao et al., 1998; Tu and Wigler, 1999; Zenke et al., 1999). For reasons that will become apparent from our description of the structure, we term part of this autoregulatory region the "inhibitory switch" (IS) domain, and we designate by "kinase inhibitor (KI) segment" a C-terminal extension of the IS domain. A dimerization (Di) segment, just upstream of the IS domain, is embedded in the PBD. PAK4, which contains a PBD but no IS domain, associates constitutively with Cdc42 (Abo et al., 1998).

Control of PAK activity depends both on the autoregulatory region in the N-terminal half of the molecule and on the state of phosphorylation of Thr423 in the kinase activation loop (Zhao et al., 1998; Zenke et al., 1999). Mutations within the autoregulatory region yield constitutively active PAK (Brown et al., 1996; Zhao et al., 1998; Tu and Wigler, 1999). Coexpression of a peptide containing residues 83–149 (that is, the IS domain and the KI segment) can inhibit PAK in *trans*, indicating a relatively tight interaction with the kinase domain (Frost et al., 1998; Zhao et al., 1998; Zenke et al., 1999).

We have made use of the observation, that PAK1(83–149) inhibits the kinase in *trans*, to form a complex between two independently expressed fragments. One of these, PAK1(70–149), we term the autoregulatory fragment; the other, PAK1(249–545), is the kinase domain. The missing segments (1–69 and 150–248) contain sites for interaction with the adaptor protein, Nck (Bokoch et al., 1996; Galisteo et al., 1996; Lu et al., 1997), and with potential downstream effector proteins of the Pix/Cool family (Bagrodia et al., 1998; Manser et al., 1998; Bagrodia and Cerione, 1999; Daniels et al., 1999). The crystal structure of this complex shows several unexpected features that are informative about PAK function in the cell. The complex is a dimer (two autoregulatory fragments and two kinase domains), held together by interaction of the autoregulatory fragments. It is a dimer in solution as well as in our crystals; the single-chain

§ To whom correspondence should be addressed (e-mail: harrison@xtal200.harvard.edu).



bound state; those in the lower bar, to the autoinhibited state. The p21 binding domain (PBD) is in red; the dimerization segment (Di), in hatched red on yellow; the inhibitory switch domain is in magenta; the kinase inhibitory segment is blue. The so-called Cdc42/Rac-interaction/binding ("CRIB") motif includes residues 75–90 (see also Figure 2B). Two other protein interaction motifs, for Nck (residues 13–21) and for PIX (182–203), are not present in our crystal structure.

species, PAK1(70–545) is also dimeric. Intact PAK1 also oligomerizes in cells (M.-C. P., M. L., and B. J. M., unpublished data). The IS domain forms the core of the autoregulatory fragment; it appears to inhibit the kinase with one surface and anchor the dimer contact with another. Its structure resembles closely that of a related, autoregulatory segment from WASP (Kim et al., 2000). As demonstrated for WASP, binding of Cdc42 or Rac to PAK will disrupt the IS domain, reconfiguring the PBD part of the autoregulatory fragment, thereby relieving the kinase inhibition and breaking the dimer contact (Abdul-Manan et al., 1999; Kim et al., 2000). The folded structure of the autoregulatory fragment is thus contingent on the identity of its partner. The PAK1 structure invokes the possibility of heterodimeric complexes of PAKs and WASPs.

## Results and Discussion

### Overview of the Structure

The preparation and crystallization of PAK1(70–149) plus PAK1(249–545) are described in Experimental Procedures. The kinase domain contains a mutation, Lys299Arg, that ablates its catalytic activity. The asymmetric unit of the crystals contains two complexes, each containing one autoregulatory fragment (residues 70–149) and one kinase domain (249–545) (Figure 2A). These are linked into a dimer by the N-terminal segments (78–88) of the autoregulatory fragments. The dimer is asymmetric, because residues 80–87, paired as antiparallel  $\beta$  strands, pack preferentially against one of the two IS domains. The conformations of the two complexes are otherwise identical, however, and the asymmetry lies entirely in different twists of the polypeptide backbone between residues 87 and 88 (Figure 3A). In the paragraphs that follow, we first describe a single autoregulatory fragment/kinase domain complex, and we then return to a description of the dimer interaction. We note that because of the chain discontinuity between residues 149 and 249, we do not yet know whether in a similar dimer with intact PAK1 chains, the regulatory contacts would be between parts of the same or of opposite polypeptides. That is, we cannot determine from the structure itself whether the regulation is in *cis* or in *trans*. We therefore designate the two autoregulatory fragments as A and B and the two kinase domains as C and D (Figure 2A). Chain A packs against C and B against D, but whether A would connect covalently to C or D in the intact dimer remains to be determined.

Figure 1. Organization of the PAK1 Polypeptide Chain

(A) The two parts of the chain used in the structure determination are shown in color. Numerals indicate residue numbers at the boundaries of various subdivisions. The autoregulatory region (70–149) is in yellow, and the kinase domain (249–545) is in blue (light blue for the N lobe; dark blue for the C lobe). The  $G_{\beta\gamma}$  binding motif at the C terminus of Ste20 is in red. The detailed substructure of the autoregulatory region is shown in the expanded lower part of the diagram. The divisions of the upper bar correspond to the p21-

### The Autoinhibited Kinase

#### The Inhibitory Switch Domain

The IS domain is a bundle of three  $\alpha$  helices ( $\alpha$ 1–3), with a short N-terminal  $\beta$  hairpin. The first strand of the hairpin is a continuation of the dimer-forming strand. The kinase inhibitor (KI) segment, which passes through the cleft of the kinase, is a C-terminal extension of the IS domain. The IS domain has a hydrophobic core, to which residues from the  $\beta$  hairpin and all three helices contribute (Figure 3A). Its structure is strikingly similar to that of the recently published "autoinhibited state of the WASP PBD" (Kim et al., 2000). Indeed, the ordered parts of the WASP fragment studied in that work (WASP residues 242–310 fused by a short linker to residues 461–492) can now be described as an IS domain (250–310) fused to an  $\alpha$  helix from the WASP cofilin-like segment (461–479). The WASP IS domain has a fourth  $\alpha$  helix at its C-terminal end.

In our PAK1 structure, helices  $\alpha$ 2 and  $\alpha$ 3 of the IS domain pack against the large lobe of the kinase (helices EF and G), with a hydrophobic interface reinforced by peripheral polar contacts. The interaction with helix G closely resembles that of the WASP IS domain with the cofilin-like helix (Figure 3B). Among the residues that contribute to the interface in PAK1 are Leu107 in helix  $\alpha$ 1, Glu116 in  $\alpha$ 2, and Asp126 in helix  $\alpha$ 3 (Figure 3C); mutations at these positions lead to constitutively active kinases (Brown et al., 1996; Zhao et al., 1998; Tu and Wigler, 1999). The tight interaction of the IS and kinase domains, disrupted by these mutations, is thus essential for positioning the KI segment across the catalytic site and for preventing activation of the enzyme. Efforts to prepare the PAK1(70–149) fragment in the absence of the kinase domain yield a poorly behaved protein with a strong tendency to aggregate. The IS domain on its own may be largely unfolded, requiring an interface with the kinase domain for stability.

#### Kinase Domain

The kinase domain has the standard, two-lobe structure characteristic of all known protein kinases (Figure 2A) (Knighton et al., 1991). There are two additional helices at the N terminus of the small lobe, and there is a final, C-terminal helix packed against the interdomain hinge. The cleft between the two lobes is relatively open. The entire small lobe is substantially more mobile than the large lobe, and several loops are particularly flexible. Helix C is displaced from the catalytic site by about 10 Å, relative to the position it is likely to have in the active conformation (Figure 4A). It appears to be stabilized in this position by interactions with helix A, which

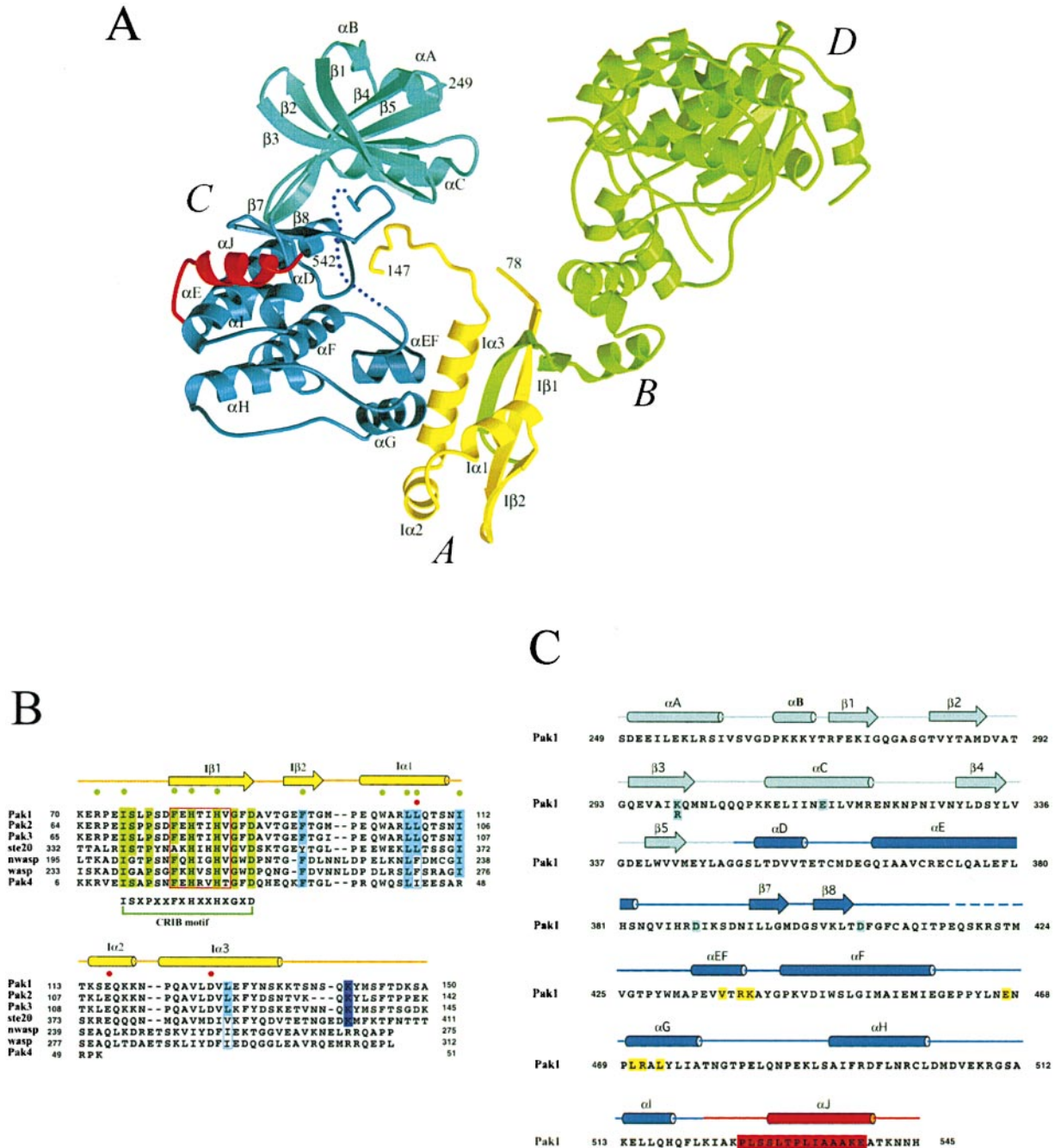


Figure 2. Overview of the PAK1 Structure

(A) Ribbon diagram of dimeric PAK1. One PAK complex, chains A and C, is colored as in Figure 1. The other, chains B and D, is in green. Chains A and B are autoregulatory regions; chains C and D are kinase domains. Secondary structures ( $\beta$  strands and  $\alpha$  helices) are labeled. The  $\alpha$  carbons of residues 88–147 in the A and B chains (the two IS domains) have a root-mean-squared deviation after superposition of 1.17 Å. The dotted line in chain C represents the disordered activation loop (416–424) in the kinase domain.

(B) Amino acid sequence alignment of the autoregulatory regions of PAK family members together with WASP and N-WASP. The alignment with WASP is based on the NMR structure (Kim et al., 2000). Secondary structure assignments from our PAK1 crystal structure are shown as colored cylinders ( $\alpha$  helices) and arrows ( $\beta$  strands) above the aligned sequences. The letter “I” in the label represents “inhibitory”. Green dots denote the residues important for association with Cdc42. The red box shows the dimerization strand; conserved residues in the so-called CRIB motif are in green; residues that interact with the kinase domain in PAK1 are in blue. Cdc42 binding will disrupt the interaction between the autoregulatory region and the kinase domain. The dark blue block shows the lysyl residue that interacts with the catalytic loop and blocks the active site of the kinase. Red dots indicate residues mentioned in text whose mutation results in activation of the kinase.

(C) Amino acid sequence of PAK1 kinase domain. Secondary structure assignments from our PAK1 crystal structure are shown as colored cylinders ( $\alpha$  helices) and arrows ( $\beta$  strands) above the aligned sequences. The lettering is consistent with Knighton et al. (1991); there are two extra N-terminal  $\alpha$  helices, which we have called  $\alpha$ A and B. The broken line shows the disordered part of the activation loop (416–425). Letters in blue blocks are important catalytic residues. In our structure, Lys299 was mutated to arginine. Letters in yellow blocks are residues that interact with the IS domain. The red block at the C terminus shows the residues in Ste20 that are believed to contact  $G_{\beta\gamma}$ .

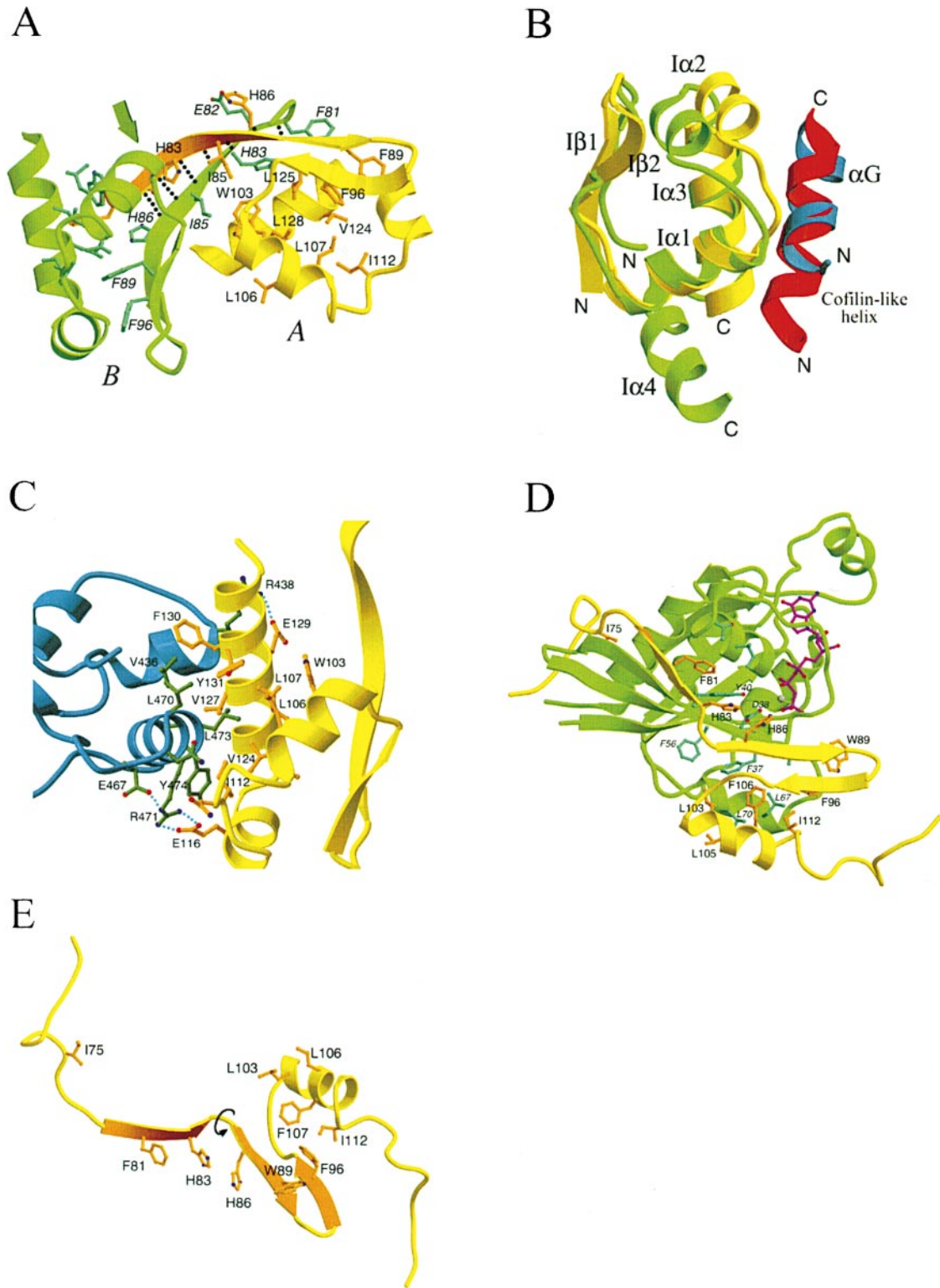
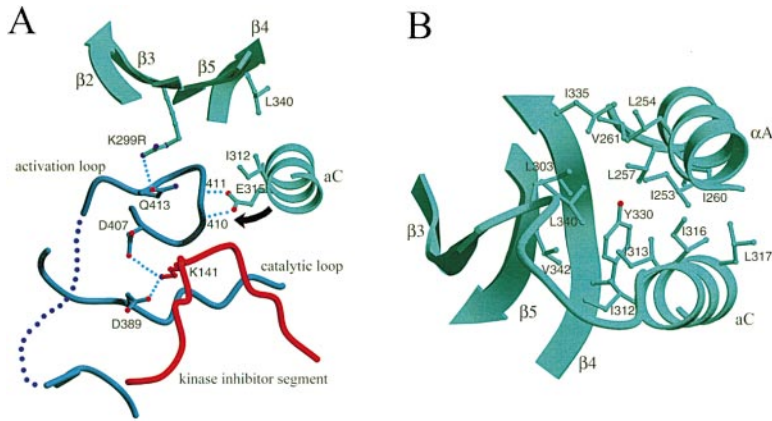


Figure 3. The IS Domain of PAK1

(A) Detailed view of the dimer interaction. (To orient with respect to Figure 2A, imagine taking the center part of that diagram and rotating it first by 90° counterclockwise and then by 90° about a horizontal axis, bringing the top out of the page.) Chain A is in yellow, chain B, in green. Black dotted lines show main chain hydrogen bonds between the two  $\beta$  strands of the dimerization segment. Side chains of residues important for dimerization and IS domain folding are shown explicitly. Labels for residues in chain B are in italics, to differentiate them from residues in chain A. To illustrate the conformational change in Pak before and after binding with GTP-Cdc42, we use different colors (yellow and orange) for the opposite sides of the  $\beta$  strand of chain A, and this convention is also used in (D) and (E). Green arrow indicates edge of strand likely to be site of attack by GTP-Cdc42 and Rac1.



strands 4 and 5 stabilize helix C in the inhibited conformation. The inner sides of helices A and C and strands 4 and 5 form a highly hydrophobic core. We expect that without helix A the small lobe of the kinase domain would not be stable.

shares a considerable hydrophobic interface with it (Figure 4B). Glu315, in the middle of helix C, would, by analogy with all other protein kinases, interact with Lys299 in the catalytic site (mutated to Arg in this “kinase-dead” form) (Johnson et al., 1996). Instead, Glu315 receives hydrogen bonds from two main chain amides (410 and 411) in the N-terminal part of the activation loop, which turns toward the rear of the catalytic site cleft and then loops forward. The position of the activation loop prevents the contacts between lobes needed to establish the active state of the enzyme and enforces the displacement of helix C by intervening between it and the catalytic residues. It also blocks part of the ATP binding site. The activation loop thus adopts a specific, inhibitory conformation, reminiscent of (but not identical to) the conformation of the homologous loop in the inactive states of c-Src and Cdk2 (De Bondt et al., 1993; Xu et al., 1999). Displacement of helix C and deconstruction of the catalytic site are clearly quite general modes for switching off protein kinase activity. The activation loop in our PAK1 structure is disordered between residues 417 and 424, including Thr423, the site of phosphorylation in active PAK1 (Zenke et al., 1999). The reasons for inaccessibility of this residue to activating kinases are not immediately evident from our structure, however.

The KI segment (residues 138 to 147) crosses the outer part of the cleft. It interacts with the activation loop between residues 407 and 413, probably stabilizing the loop’s inhibitory conformation. Lysine 141 projects

directly toward the catalytic residues, forming salt bridges with both key aspartates (Asp389 and Asp407). Three hydrophobic residues, Tyr142, Met143, and Phe145 also contribute to the displacement of helix C.

At the C terminus of the kinase domain is an  $\alpha$  helix, not found in most other kinases, which packs against the interdomain hinge (Figure 2A). The corresponding C-terminal sequence of Ste20 has been identified as a target for regulation by  $G_{\beta\gamma}$  in signaling from the yeast pheromone receptor (Leeuw et al., 1998). The position of the C-terminal helix seen in our structure would prevent the small lobe from moving into its active-state orientation.

#### The Dimer

The core of the dimer interaction is an antiparallel  $\beta$  ribbon, formed by residues 80–87 from each of the two monomers (Figure 3A). Seven main chain hydrogen bonds link the two segments, and there are salt bridges between Glu82 on one strand and His86 on the other. The paired strands pack preferentially against IS domain A (IS-A). The chains are so disposed that strand  $\beta$ 1-B is clamped between strand  $\beta$ 1-A and the rest of IS-A. Hydrophobic contacts of Phe81-B with Pro121-A and Leu125-A and of Ile85-B with Pro100-A and Trp103-A appear to stabilize the asymmetric packing. Any fully symmetric structure would leave Phe81 and Ile85 exposed to solvent. In solution, the dimer presumably can

Figure 4. The Inhibited Conformation of PAK1 Kinase Domain

(A) The inhibited active site of PAK1. The view is from the right of the C chain in Figure 2A. The KI segment of the autoregulatory fragment occupies the cleft between the N lobe and the C lobe of the kinase domain. Lys141 makes hydrogen bonds with Asp389 of the catalytic loop and Asp407 of the activation loop. Asp389 is the catalytic base in an active kinase. The activation loop is forced to make a turn (407–413), which blocks the contact between Glu315 of Helix C and K299R and prevents binding of ATP. The arrow indicates the shift in helix C that would be required for it to move to its expected position in an active enzyme.

(B) Hydrophobic contacts from helix A and

(B) Superposition of the IS domain and helix  $\alpha$ G of PAK1 on the NMR structure of the WASP IS domain linked to a C-terminal, “cofilin-like” helix (Kim et al., 2000). PAK is in yellow and blue and WASP in green and red. The PAK1 and WASP IS domains both include a  $\beta$  hairpin ( $\beta$ 1–2) and three  $\alpha$  helices ( $\alpha$ 1–3; WASP has an extra helix,  $\alpha$ 4). The stability of the IS domain appears to require that another  $\alpha$  helix ( $\alpha$ G in PAK1; the cofilin-like helix in WASP) bind on the side of the IS domain opposite to the  $\beta$  hairpin.

(C) Interactions between the IS and kinase domain. The view corresponds to the chain A–chain C contact in Figure 2A. Asp126 (not labeled) is on the rear of  $\alpha$ 3.

(D) The NMR structure of a complex of Cdc42 and the WASP PBD, drawn from the coordinates of Kim et al. (2000). For clarity, we use PAK1 numbering for the equivalent residues in WASP. Cdc42 is in green; the WASP PBD, in yellow. GMPCP bound to Cdc42 is in magenta, and the  $Mg^{2+}$  is gray. A  $\beta$  strand of WASP augments the central  $\beta$  sheet of Cdc42, but note that a  $\beta$  bulge between His83 and His86 of WASP places these residues on the same side of the strand. The IS domain is partially unfolded by Cdc42.

(E) The WASP PBD domain, extracted from the Cdc42-WASP complex in (D) and rotated to correspond to the orientation of the N-terminal part of the yellow  $\beta$  strand in (A). The view is essentially as if looking outward from within Cdc42. Comparing this drawing with (A), we can describe as follows the conformational change in the PBD domain of PAK1 that accompanies binding with Cdc42. Viewed as in A, Cdc42 approaches from the upper left (arrow in A) and associates first with the N-terminal part of the PBD (residues 70–84) to form a hybrid  $\beta$  sheet. Then the rest of the PBD domain (residues 85–136) rotates by  $\sim 180^\circ$  around the backbone of residue Thr84 to form a  $\beta$  bulge (arrow). In this process, helices  $\alpha$ 2,  $\alpha$ 3 and (in WASP)  $\alpha$ 4 unfold.

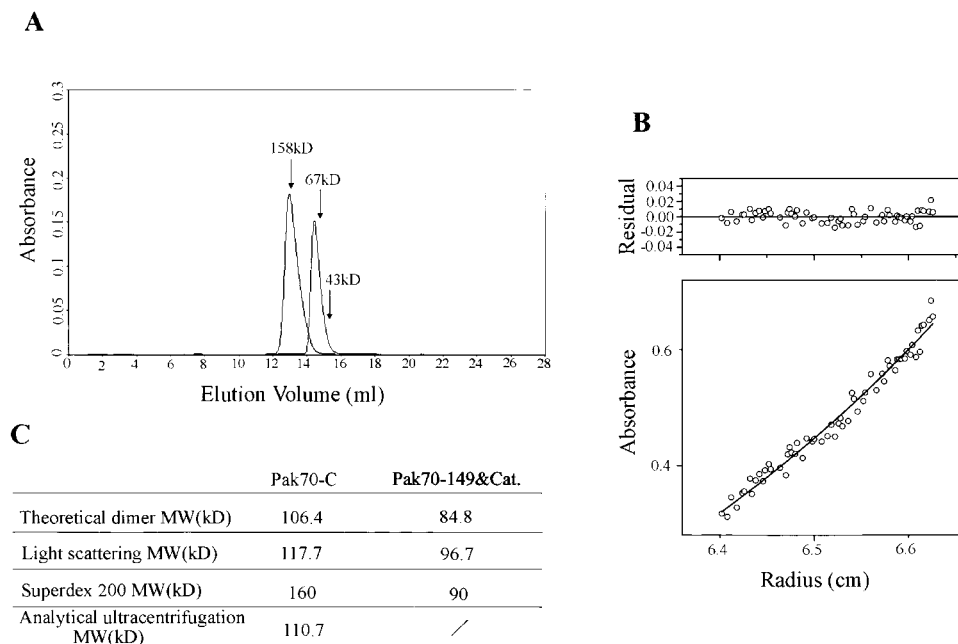


Figure 5. PAK1 Forms a Dimer in Solution

(A) Gel filtration profiles on Superdex200 (Pharmacia) for PAK1(70–545) and for PAK1(70–149) plus PAK1(249–545). Elution positions for three calibration standards are shown. Pak70-C elutes at a position corresponding to a relative molecular mass of 160 kDa, larger than the expected dimer mass of 110 kDa, probably due to an extended loop formed by residues 150–248. The two-chain complex we have crystallized elutes with an apparent relative molecular mass of 90 kDa, consistent with the expected size of a dimer (85 kDa).

(B) Sedimentation equilibrium analysis of PAK1(70–545) was carried out using an Optima XL-A analytical ultracentrifuge (Beckman). Experiments were performed at 4°C at 16,000 rpm with protein concentrations of ~0.6, 0.3, and 0.15 mg/ml. The data (open circles) fall on a curve (lower panel) that describes the concentration distribution of a single, ideal species (Beckman). The residuals for this fit are shown in the upper panel.

(C) Summary of experiments showing that PAK1 forms a dimer in solution. Dynamic light scattering measurements were performed with a DynaPro-810 dynamic-light-scattering molecular-size detector (PROTEINSOLUTIONS).

flip back and forth between two equivalent asymmetric states, with hinge points at Val87 (A and B).

What is the oligomeric state of PAK1 in solution? As summarized in Figure 5, experiments using calibrated size exclusion chromatography, dynamic light scattering, and analytical ultracentrifugation demonstrate that PAK1(70–149 + 249–545) and PAK1(70–545) are assemblies of about 85 kDa and 106 kDa, respectively, as expected if the crystallographic interaction is present in these species. The hydrodynamic radius of the PAK1(70–545) dimer is significantly larger than that of the four-chain complex, probably because residues 150–248 are in an extended, flexible loop with measurable frictional drag. PAK1 can also dimerize when expressed in 293 cells, and these dimers dissociate when coexpressed with activated Cdc42 or Rac1 (M.-C. P., M. L., and B. J. M., unpublished data).

#### Activation by Cdc42

We can model how Cdc42 might interact with PAK1, by referring to the published solution structure of the WASP PBD complexed with Cdc42:GTP (Abdul-Manan et al., 1999). [After this paper was completed, two solution structures of the PAK1 PBD bound with Cdc42:GTP appeared (Morreale et al., 2000; Gizachew et al., 2000). The better determined of the two (Morreale et al., 2000) coincides in all critical respects with the WASP:Cdc42 complex. We believe that the latter is somewhat more

accurate in a key comparison region, and we have therefore chosen to use it, rather than the PAK1 complex, for comparison.] The WASP peptide in the complex (residues 230–288) corresponds to residues 67–125 of PAK1 (see Figure 2B); for simplicity we use PAK1 numbering here to describe the interactions. Residues 67–113 are well defined (Figure 3D). Residues 79–84 form a  $\beta$  strand, which adds to the edge of the Cdc42  $\beta$  sheet. Unlike  $\text{I}\beta 1$  in the PAK1 dimer, however, the  $\text{I}\beta 1$  strand in the WASP-Cdc42 complex does not continue smoothly into a  $\beta$  hairpin. Rather, there is a  $\beta$  bulge at residue 85, followed by a hairpin (equivalent to the hairpin in PAK1 formed by the C-terminal part of  $\text{I}\beta 1$  and  $\text{I}\beta 2$ ) and then by an  $\alpha$  helix ( $\text{I}\alpha 1$ ). The effect of the bulge is to flip the polypeptide chain by  $\sim 180^\circ$  around its axis, relative to the unbulged strand in PAK1, and part of the Cdc42  $\beta$  interaction is thus on the opposite side of the strand from the  $\beta$  ribbon interaction in the PAK1 dimer (compare Figures 3A and 3E). The  $\beta$  hairpin and  $\text{I}\alpha 1$  are also more separated in WASP-Cdc42 than in PAK1, and it would not be possible to fold  $\text{I}\alpha 2$  and  $\text{I}\alpha 3$  into the Cdc42 complex without collisions. Thus, we expect Cdc42 binding to unfold part of the IS domain and to dissociate the dimer. In their report, described above, on the solution structure of the WASP PBD/IS region, Kim et al. (2000) conclude that interaction with Cdc42 will likewise disrupt the fold of the WASP IS domain.

It is possible to imagine that Cdc42 begins by contacting the N-terminal part of  $\text{I}\beta 1$ , approaching from the

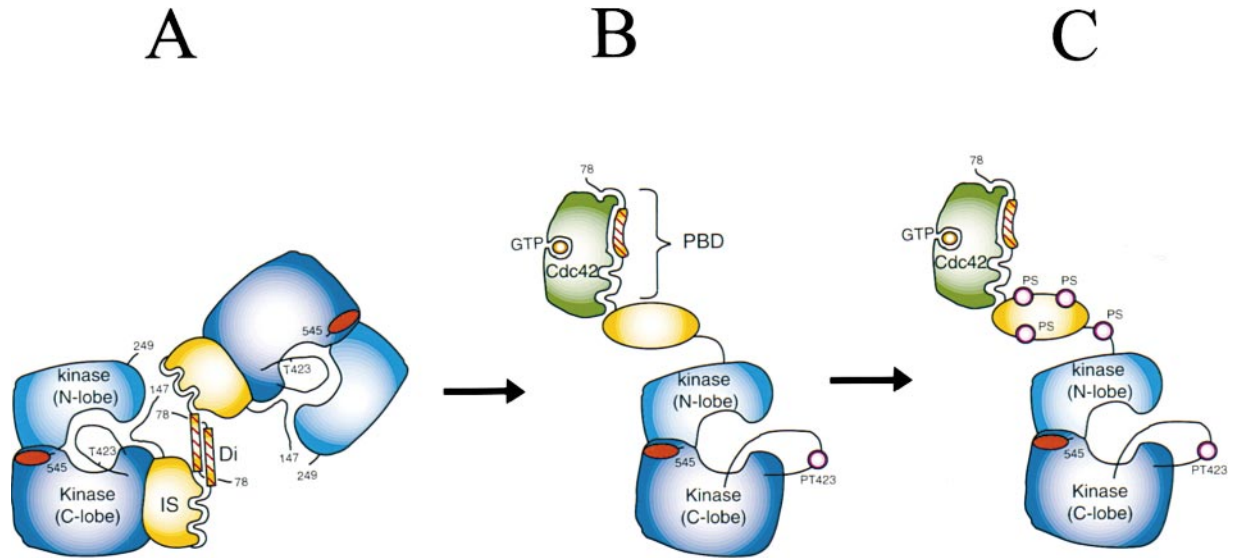


Figure 6. Model for PAK1 Activation

(A) In the autoinhibited conformation, PAK1 is an asymmetric dimer. The inhibitory switch (IS) domain associates tightly with the C lobe of the kinase domain. The kinase inhibitory (KI) segment (137–149) occupies the cleft of the kinase domain and stabilizes a disabled catalytic site. The color scheme for PAK1 matches that in Figure 1. Numerals indicate residue numbers. The connections between residues 147 and 249 in the two partners are not shown, because we do not yet know whether the links are made in *cis* or in *trans*.

(B) Binding of GTP-loaded Cdc42 (or Rac) with the PAK1 p21 binding domain (PBD) disrupts the dimer and unfolds the IS domain (symbolized by its reversion to a formless oval). The conformational change withdraws the KI segment from the cleft of the kinase domain and releases the activation loop. Phosphorylation of Thr423 (PT423) will activate the enzyme.

(C) Once Thr423 has been phosphorylated, PAK can autophosphorylate at several sites (phosphoserine: PS) within the first 250 amino acids. These modifications prevent the kinase from reverting to an inactive conformation.

free edge of chain A (chain B is less accessible), and to imagine further that Cdc42 then invades and disrupts the autoregulatory region and dissociates the dimer (Figures 3A and 3E). This rearrangement would be driven by the extensive contacts between Cdc42 and the parts of the IS domain (the  $\beta$  hairpin and  $I\alpha 1$ ) that remain structured in the final complex.

#### Two States of the PBD/IS Region

In the two states of the WASP PBD/IS region studied by NMR (Abdul-Manan et al., 1999; Kim et al., 2000), an ordered structure (the IS domain) in one state partly but incompletely overlaps with an ordered structure (the PBD, as defined by the Cdc42 complex) in another state. The same holds for the PAK1 PBD/IS region, under the reasonable assumption that the interaction of PAK1 with Cdc42 resembles that of WASP (Figures 3A and 3E). We term this phenomenon, in which alternative folded states of a protein segment depend on its interactions with other proteins or with another part of its own polypeptide chain, “contingent folding.” Moreover, as documented for the WASP PBD/IS region and suggested by the instability in solution of PAK1(70–149), the contingently folded segment may be fully disordered in the absence of interaction with other protein elements. Kim et al. (2000) have shown that the fused cofilin-like segment is required to obtain a fully folded WASP IS structure, unless small amounts of organic solvent are used to stabilize its largely helical secondary-structure elements. The marginal stability of one state of a contingently folded domain may be essential for its capacity to switch into another state.

The PAK1 structure shows a further level of complexity, because part of the PBD is also a dimerizing motif. In one member of the dimer, the IS domain interacts only with the large lobe of a kinase; in the other, it also interacts with the paired  $\beta$  strands of the dimerization element. We infer that contacts with the kinase domain are sufficient to stabilize the PAK1 IS fold, and that the IS domain can in turn stabilize pairing of the dimerization segments. The folded domain is thus an inhibitory switch in three senses: it positions the KI segment in the mouth of the kinase; it interferes with Cdc42 binding; it cements the dimer contact.

The central role of the IS domain in mediating activation by Cdc42 or Rac is illustrated in the model for PAK1 activation drawn in Figure 6. Binding of the GTP-loaded small GTPase reconfigures the PBD and unfolds the IS domain. The unfolded IS domain and the KI segment dissociate from the kinase, which can then be activated by phosphorylation of Thr423. Subsequent phosphorylation of serines within the KI region (and perhaps the IS region) prevents any simple reversal of the activation steps (Manser et al., 1997; Gatti et al., 1999).

#### Dimers, Heterodimers, and PAK1 Autoregulation

Is dimerization required for PAK1 autoinhibition? The structure reported here cannot resolve this question, because of the missing connection between the two fragments. The linker between the autoregulatory region and the kinase domain contains 99 residues, and it is long enough to make either a *cis* or a *trans* connection. Indeed, both possible connections could in principle be present in a population of PAK1 dimers. If the interaction

Table 1. Data Collection, Phase Determination, and Refinement Statistics

Crystal	Native	MeHgNO <sub>3</sub>			
Resolution (Å)	50–2.3	45–2.8			
R <sub>sym</sub>	6.9%	7.6%			
Total Observations	160,255	193,639			
Unique observations	56,384	32,075			
Coverage	98.2%	99.7%			
No. of sites		4			
Phasing power (12–2.8 Å, SAD)		0.52			
R <sub>cullis</sub> (%; 12–2.8 Å, ano)		0.96			
Figure of merit		0.12			
Wavelength (Å)		1.000			
Refinement					
R <sub>free</sub> (%; 50–2.3 Å)	25.8				
R <sub>cryst</sub> (%; 50–2.3 Å)	23.7				
		Rmsd			
	Res. no.	Average B	Bonds (Å)	Angles (°)	B Values (Å <sup>2</sup> bonded)
Protein	712	56.6	0.006	1.32	1.27
Iodide	28	52.5			
Water	582	66.3			

$R_{\text{sym}} = \sum |I - \langle I \rangle| / \sum I$ , where  $I$  is the observed intensity,  $\langle I \rangle$  is the average intensity of multiple observations of symmetry-related reflections.  $R_{\text{cullis}} (\text{ano}) = \sum |F_{\text{PH}+} - F_{\text{PH}-}| \exp[-|F_{\text{PH}+} - F_{\text{PH}-}| \text{calc}] / \sum |F_{\text{PH}+} - F_{\text{PH}-}| \exp$ , where  $F_{\text{PH}}$  is the heavy-atom derivative structure factor amplitude. Phasing power =  $\text{rms.} (|F_{\text{H}}|/E)$ , where  $|F_{\text{H}}|$  is the heavy-atom structure factor amplitude and  $E$  is the residual lack of closure error. Figure of merit =  $\langle \sum P(\alpha) e^{i\alpha} / \sum P(\alpha) \rangle$ , where  $\alpha$  is the phase and  $P(\alpha)$  is the phase probability distribution.  $R = \sum |F_{\text{o}}| - |F_{\text{c}}| / \sum |F_{\text{o}}|$ , where  $F_{\text{o}}$  and  $F_{\text{c}}$  are observed and calculated structure factor amplitudes, respectively.  $R_{\text{free}}$  is calculated for a randomly chosen 5% of reflections;  $R_{\text{cryst}}$  is calculated for the remaining 95% of reflections used for structure refinement. Rmsd is the root mean square derivation from ideal geometry.

between an IS domain and a kinase domain in a dimer of intact PAK1 is *trans*, then dimerization will obviously be necessary to establish an inhibited state. If the interaction is *cis*, then formation of the dimer may help stabilize the IS fold and thereby enhance inhibition, but it will probably not be essential. The linker contains a binding site for proteins of the Pix/Cool family (Bagrodia et al., 1998; Manser et al., 1998; Bagrodia and Cerione, 1999). These proteins could influence the stability of the inhibited state by a variety of mechanisms, including a shift in the balance between *cis* and *trans* connections.

The observation that a segment of the PAK1 PBD can also be a dimerization element suggests that other PBD/IS-containing proteins might dimerize and that heterodimers might form as well. The dimerization segment itself, immediately N-terminal to the IS domain, is one of the most conserved parts of the PBD; indeed, it corresponds essentially to the sequence often called the "CRIB motif" (Figures 1 and 2B) (Burbelo et al., 1995). We note, however, that the fragment of WASP that includes the PBD and the IS domain appears to be monomeric in solution (Kim et al., 2000), and preliminary measurements on intact, recombinant N-WASP give no evidence for dimerization (M. L. and R. Rohatgi, unpublished).

Our structure suggests that dimerization requires both the short segment containing PAK1 residues 78–87 and an intact IS domain. PAKs1–3, WASP, and N-WASP all meet this requirement. The regulatory region of PAK4 terminates at the equivalent of PAK1 residue 115, however, and it thus has a PBD but not a full IS domain (see alignment in Figure 2B). ACK and MIHCK also have PBDs without complete IS domain sequences (Manser et al., 1993; Yang and Cerione, 1997; Abo et al., 1998; Brzeska et al., 1999). If the sequences of complete IS domains are used in standard database searches, only members

of the PAK and WASP families appear consistently, but related structures may fold from sequences with currently undetectable relationship to PAKs or WASPs or from sequences not yet in the protein databases.

The functional consequence of heterodimerization among members of the PAK and WASP families would be to create a hierarchically interconnected network of proteins that bind Cdc42 and Rac on the one hand and that interact with actin or with Arp2/3 on the other. Not all possible hetero- or homodimers would be equally likely, just as in the Fos/Jun family of heterodimerizing transcription factors, only specific combinations are stable (Smeal et al., 1989). The interactions generated by such a network would produce unexpectedly elaborate ways to modulate organization of the actin cytoskeleton.

## Conclusions

PAK1 is regulated by overlapping control elements. The structural realization of this regulation is a marked departure from the simple modularity sometimes assumed for signaling proteins. The structure shows that an inhibitory switch domain, also present in WASP family proteins (Kim et al., 2000), folds in association with the large lobe of the kinase. The IS domain bears a C-terminal extension which directly blocks the kinase catalytic cleft, and an N-terminal extension which dimerizes the protein. GTP-bound Cdc42 or Rac interacts with a segment of PAK1 (the PBD) that overlaps the dimerization element and part of the IS domain. From the structure of a Cdc42/WASP complex (Abdul-Manan et al., 1999), we anticipate that Cdc42 or Rac will dissociate the dimer, refold part of the IS domain and unfold the rest, thereby disrupting IS-kinase contacts and withdrawing the inhibitory segment from the catalytic cleft of the enzyme. Contingent folding of the IS domain makes

possible the overlap of control elements. Dimerization, mediated by part of the PBD and anchored by the kinase-associated state of the IS domain, provides an unanticipated further level of regulatory complexity.

#### Experimental Procedures

##### Protein Expression and Purification

The autoregulatory fragment (residues 79–149) and the kinase domain (residues 249–545) of human PAK1 were cloned into the GST-fusion vector pGEX2N (Pharmacia), with a thrombin site C-terminal to the GST moiety, and expressed in *E. coli*/NB42. The kinase domain contained the inactivating mutation K299R, because the wild-type form proved toxic to bacterial cells. Both GST-PAK1(70–149) and GST-PAK1(249–545) were induced by 0.1 mM IPTG at  $OD_{600} = 0.6$ . GST-PAK1(70–149) was expressed for 6 hr, 28°C. Cells were lysed by sonication in 150 mM NaCl, 25 mM Tris-HCl, pH 8.0 (buffer A) with 5 mM benzamidine and 5 mM DTT. Lysates were applied to Glutathione sepharose-4B columns and eluted with 15 mM glutathione. GST-PAK1(249–545) was incubated with thrombin (1000 units/ml) for 12 hr, room temperature, mixed with GST-PAK(70–149), and incubated for another 6 hr with freshly added thrombin. Glutathione was removed by passing the protein solution through a PD-10 column (Pharmacia) and GST was removed by passage through Glutathione-4B. The PAK1(70–149)-PAK1(249–545) complex was purified by passage through Mono-Q and by size-exclusion chromatography on Superdex 200 equilibrated with 125 mM NaCl, 20 mM Tris-HCl, pH 8.0 (Buffer B). This procedure typically yielded 15–20 mg PAK complex from 2 liters of cell culture for each of the two constructs.

##### Crystallization and X-Ray Data Collection

Crystals were grown by hanging-drop vapor diffusion by equilibrating against 1.8–1.9 M  $(NH_4)_2SO_4$ , 150 mM NaCl, 250–300 mM NaI, 10 mM DTT, 100 mM PIPES, pH 6.5 (well solution), a drop containing 3  $\mu$ l protein solution in buffer B plus 3  $\mu$ l well solution. The crystals grew to 0.1–0.2 mm size in about 5 days at 12°C. They are in space group P41,  $a = b = 94.58$  Å,  $c = 147.50$  Å, with two PAK1 complexes per asymmetric unit. For preparation of a mercury derivative, crystals were transferred gradually into 2.0 M  $(NH_4)_2SO_4$ , 150 mM NaCl, 200 mM  $NaNO_3$ , 10 mM DTT, 100 mM PIPES, pH 6.5, and soaked in this buffer with 1 mM added  $CH_3HgNO_3$ . For data collection at low temperature, crystals were transferred stepwise into a stabilizing solution containing 25% glycerol, 2.0 M  $(NH_4)_2SO_4$ , 125 mM NaCl, 100 mM PIPES, pH 6.5, 250 mM NaI (native) or 100 mM  $NaNO_3$  (derivative). The crystals were flash frozen by immersion in liquid nitrogen. Diffraction data were collected at APS beamline BM 14-C using a Quantum-4 detector. Data (Table 1) were integrated and scaled using the HKL programs (DENZO and SCALEPAK) (Otwinowski, 1993).

##### Structure Determination and Refinement

Single-wavelength anomalous dispersion (SAD) data from the mercury derivative were used to obtain initial phases. Four mercury atoms were located by anomalous Patterson and difference Fourier methods, using the CNS suite (Brünger et al., 1998). Mercury positions were refined and SAD phases calculated using CNS; the initial SAD map was significantly improved by solvent flattening. Skeletonization of the improved map with MAPMAN (Kleywegt and Jones, 1994) allowed us to fit a model of the cAPK kinase domain as a rigid body and then to extend the trace to the two autoregulatory regions within the asymmetric unit. From this rough initial model, the noncrystallographic symmetry (NCS) transformations were calculated (separately for the IS domain, residues 88–147, and for the N and C lobes of the kinase domain); another round of density modification, combining solvent flattening, histogram matching, and 2-fold NCS averaging, led to a very clear and completely interpretable map. A model of the relevant residues of human PAK1 was built into the density using the program O (Jones et al., 1989); the model was then transferred into the native unit cell by rigid-body refinement and further refined using simulated-annealing and positional refinement (CNS), with manual rebuilding (O). Simulated-annealing OMIT maps were computed to check the conformations of the two autoregulatory fragments. The refined model includes

residues 78–147, 249–415, and 423–542 in complex A/C, residues 78–147, 249–416, and 426–542 in complex B/D, plus 28 iodide ions and 582 water molecules in the asymmetric unit. Over 99% of the residues are in the two “most favored” regions of a Ramachandran diagram; none are in forbidden regions. The average thermal parameters for the IS domains and for the large lobes of the kinase domains are quite similar (45–55 Å<sup>2</sup>); the small lobes of the kinase domains are more mobile (70–80 Å<sup>2</sup>). The coordinates have been deposited at the RCSB Protein Data Bank (ID code 1F3M).

##### Illustrations

Figures were prepared using MolScript (Kraulis, 1991) and Raster3D (Merritt and Murphy, 1994).

##### Acknowledgments

We thank Wilfried Schildkamp and the staff of beamline 14-C at BioCARS (APS) for assistance with data collection, A. Carfi, G. Zhou, G. Gao, and X. Huang for help at various stages of the project, and M. K. Rosen (Sloan-Kettering Institute) for coordinates and thoughtful discussions. We acknowledge support from NIH grant 1R01 CA2258-01 from the NCI (to B. J. M.). This is a contribution from the Harvard-Armenise Center for Structural Biology. S. C. H. is an Investigator of the Howard Hughes Medical Institute.

Received May 3, 2000; revised June 13, 2000.

##### References

- Abdul-Manan, N., Aghazadeh, B., Liu, G.A., Majumdar, A., Ouerfelli, O., Siminovitich, K.A., and Rosen, M.K. (1999). Structure of Cdc42 in complex with the GTPase-binding domain of the ‘Wiskott-Aldrich syndrome’ protein. *Nature* **399**, 379–383.
- Abo, A., Qu, J., Cammarano, M.S., Dan, C., Fritsch, A., Baud, V., Belisle, B., and Minden, A. (1998). PAK4, a novel effector for Cdc42Hs, is implicated in the reorganization of the actin cytoskeleton and in the formation of filopodia. *EMBO J.* **17**, 6527–6540.
- Bagrodia, S., and Cerione, R.A. (1999). Pak to the future. *Trends Cell Biol.* **9**, 350–355.
- Bagrodia, S., Derijard, B., Davis, R.J., and Cerione, R.A. (1995). Cdc42 and PAK-mediated signaling leads to Jun kinase and p38 mitogen-activated protein kinase activation. *J. Biol. Chem.* **270**, 27995–27998.
- Bagrodia, S., Taylor, S.J., Jordon, K.A., Van Aelst, L., and Cerione, R.A. (1998). A novel regulator of p21-activated kinases. *J. Biol. Chem.* **273**, 23633–23636.
- Bokoch, G.M., Wang, Y., Bohl, B.P., Sells, M.A., Quilliam, L.A., and Knaus, U.G. (1996). Interaction of the Nck adapter protein with p21-activated kinase (PAK1). *J. Biol. Chem.* **271**, 25746–25749.
- Brown, J.L., Stowers, L., Baer, M., Trejo, J., Coughlin, S., and Chant, J. (1996). Human Ste20 homologue hPAK1 links GTPases to the JNK MAP kinase pathway. *Curr. Biol.* **6**, 598–605.
- Brünger, A.T., Adams, P.D., Clore, G.M., Delano, W.L., Gros, P., Grosse-Kuntze, R.W., Jiang, J.-S., Kyszewski, J., Nilges, M., Pannu, N.S., et al (1998). Crystallography and NMR system: a new software suite for macromolecular structure determination. *Acta Crystallogr. D* **54**, 905–921.
- Brzeska, H., Knaus, U.G., Wang, Z.Y., Bokoch, G.M., and Korn, E.D. (1997). p21-activated kinase has substrate specificity similar to Acanthamoeba myosin I heavy chain kinase and activates Acanthamoeba myosin I. *Proc. Natl. Acad. Sci. USA* **94**, 1092–1095.
- Brzeska, H., Young, R., Knaus, U., and Korn, E.D. (1999). Myosin I heavy chain kinase: cloning of the full-length gene and acidic lipid-dependent activation by Rac and Cdc42. *Proc. Natl. Acad. Sci. USA* **96**, 394–399.
- Bubeck-Wardenburg, J., Pappu, R., Bu, J.Y., Mayer, B., Chernoff, J., Straus, D., and Chan, A.C. (1998). Regulation of PAK activation and the T cell cytoskeleton by the linker protein SLP-76. *Immunity* **9**, 607–616.
- Burbelo, P.D., Drechsel, D., and Hall, A. (1995). A conserved binding

- motif defines numerous candidate target proteins for both Cdc42 and Rac GTPases. *J. Biol. Chem.* **270**, 29071–29074.
- Buss, F., Kendrick-Jones, J., Lionne, C., Knight, A.E., Cote, G.P., and Paul Luzio, J. (1998). The localization of myosin VI at the golgi complex and leading edge of fibroblasts and its phosphorylation and recruitment into membrane ruffles of A431 cells after growth factor stimulation. *J. Cell Biol.* **143**, 1535–1545.
- Cullen, B.R. (1996). HIV-1: is Nef a PAK animal? *Curr. Biol.* **6**, 1557–1559.
- Daniels, R.H., and Bokoch, G.M. (1999). p21-activated protein kinase: a crucial component of morphological signaling? *Trends Biochem. Sci.* **24**, 350–355.
- Daniels, R.H., Zenke, F.T., and Bokoch, G.M. (1999). alphaPix stimulates p21-activated kinase activity through exchange factor-dependent and -independent mechanisms. *J. Biol. Chem.* **274**, 6047–6050.
- De Bondt, H.L., Rosenblatt, J., Jancarik, J., Jones, H.D., Morgan, D.O., and Kim, S.H. (1993). Crystal structure of cyclin-dependent kinase 2. *Nature* **363**, 595–602.
- Fackler, O.T., Lu, X., Frost, J.A., Geyer, M., Jiang, B., Luo, W., Abo, A., Alberts, A.S., and Peterlin, B.M. (2000). p21-activated kinase 1 plays a critical role in cellular activation by Nef. *Mol. Cell Biol.* **20**, 2619–2627.
- Frost, J.A., Xu, S., Hutchison, M.R., Marcus, S., and Cobb, M.H. (1996). Actions of Rho family small G proteins and p21-activated protein kinases on mitogen-activated protein kinase family members. *Mol. Cell Biol.* **16**, 3707–3713.
- Frost, J.A., Khokhlatchev, A., Stippec, S., White, M.A., and Cobb, M.H. (1998). Differential effects of PAK1-activating mutation reveal activity-dependent and -independent effects on cytoskeletal regulation. *J. Biol. Chem.* **273**, 28191–28198.
- Galisteo, M.L., Chernoff, J., Su, Y.C., Skolnik, E.Y., and Schlessinger, J. (1996). The adaptor protein Nck links receptor tyrosine kinases with the serine-threonine kinase Pak1. *J. Biol. Chem.* **271**, 20997–21000.
- Gatti, A., Huang, Z., Tuazon, P.T., and Traugh, J.A. (1999). Multisite autophosphorylation of p21-activated protein kinase  $\gamma$ -PAK as a function of activation. *J. Biol. Chem.* **274**, 8022–8028.
- Gizachew, D., Guo, W., Chohan, K.K., Sutcliffe, M.J., and Oswald, R.E. (2000). Structure of the complex of Cdc42Hs with a peptide derived from P-21 activated kinase. *Biochemistry* **39**, 3963–3971.
- Hing, H., Xiao, J., Harden, N., Lim, L., and Zipursky, S.L. (1999). Pak functions downstream of Dock to regulate photoreceptor axon guidance in *Drosophila*. *Cell* **97**, 853–863.
- Johnson, L.N., Noble, M.E., and Owen, D.J. (1996). Active and inactive protein kinases: structural basis for regulation. *Cell* **85**, 149–158.
- Jones, T.A., Bergdoll, M., and Kjeldgaard, M. (1989). Crystallographic Computing and Modeling Methods in Molecular Design, C. Bugg and S. Ealick, eds. (New York: Springer).
- Kim, A.S., Kakalis, L.T., Abdul-Manan, N., Liu, G.A., and Rosen, M.K. (2000). Autoinhibition and activation mechanisms of the Wiskott-Aldrich syndrome protein. *Nature* **404**, 151–158.
- Kleywegt, G.J., and Jones, T.A. (1994). From first map to final model. In *Proceedings of the CCP4 Study Weekend*, S. Bailey, R. Hubbard, and D. Waller, eds. (Daresbury, UK: Daresbury Laboratory), pp. 59–66.
- Knaus, U.G., and Bokoch, G.M. (1998). The p21Rac/Cdc42-activated kinases (PAKs). *Int. J. Biochem. Cell Biol.* **30**, 857–862.
- Knighton, D.R., Zheng, J.H., Ten Eyck, L.F., Ashford, V.A., Xuong, N.H., Taylor, S.S., and Sowadski, J.M. (1991). Crystal structure of the catalytic subunit of cyclic adenosine monophosphate-dependent protein kinase. *Science* **253**, 407–414.
- Kraulis, P.J. (1991). MOLSCRIPT: a program to produce both detailed and schematic plots of protein structure. *J. Appl. Crystallogr.* **24**, 946–950.
- Leeuw, T., Wu, C., Schrag, J.D., Whiteway, M., Thomas, D.Y., and Leberer, E. (1998). Interaction of a G-protein beta-subunit with a conserved sequence in Ste20/PAK family protein kinases. *Nature* **391**, 191–195.
- Lim, L., Manser, E., Leung, T., and Hall, C. (1996). Regulation of phosphorylation pathways by p21 GTPases. The p21 Ras-related Rho subfamily and its role in phosphorylation signalling pathways. *Eur. J. Biochem.* **242**, 171–185.
- Lu, W., and Mayer, B.J. (1999). Mechanism of activation of Pak1 kinase by membrane localization. *Oncogene* **18**, 797–806.
- Lu, W., Katz, S., Gupta, R., and Mayer, B.J. (1997). Activation of Pak by membrane localization mediated by an SH3 domain from the adaptor protein Nck. *Curr. Biol.* **7**, 85–94.
- Manser, E., Leung, T., Salihuddin, H., Tan, L., and Lim, L. (1993). A non-receptor tyrosine kinase that inhibits the GTPase activity of p21cdc42. *Nature* **363**, 364–367.
- Manser, E., Leung, T., Salihuddin, H., Zhao, Z., and Lim, L. (1994). A brain serine/threonine protein kinase activated by Cdc42 and Rac1. *Nature* **367**, 40–46.
- Manser, E., Huang, H.Y., Loo, T.H., Chen, X.Q., Dong, J.M., Leung, T., and Lim, L. (1997). Expression of constitutively active alpha-PAK reveals effects of the kinase on actin and focal complexes. *Mol. Cell Biol.* **17**, 1129–1143.
- Manser, E., Loo, T.H., Koh, C.G., Zhao, Z.S., Chen, X.Q., Tan, L., Tan, I., Leung, T., and Lim, L. (1998). PAK kinases are directly coupled to the PIX family of nucleotide exchange factors. *Mol. Cell* **1**, 183–192.
- Merritt, E.A., and Murphy, M.E.P. (1994). Raster3D version 2.0, a program for photorealistic molecular graphics. *Acta Crystallogr. D* **50**, 869–873.
- Morreale, A., Venkatesan, M., Mott, H.R., Owen, D., Nieltispach, D., Lowe, P.N., and Laue, E.D. (2000). Structure of Cdc42 bound to the GTPase binding domain of PAK. *Nat. Struct. Biol.* **7**, 384–388.
- Otwinowski, Z. (1993). Oscillation data reduction program. In *Data Collection and Processing of Proceedings of the CCP4 Study Weekend*, L. Sawyer, N. Isaacs, and S. Bailey, eds. (Warrington, UK: SERC Daresbury Laboratory), pp. 56–62.
- Renkema, G.H., Manninen, A., Mann, D.A., Harris, M., and Saksela, K. (1999). Identification of the Nef-associated kinase as p21-activated kinase 2. *Curr. Biol.* **9**, 1407–1410.
- Rohatgi, R., Ma, L., Miki, H., Lopez, M., Kirchhausen, T., Takenawa, T., and Kirschner, M.W. (1999). The interaction between N-WASP and the Arp2/3 complex links Cdc42-dependent signals to actin assembly. *Cell* **97**, 221–231.
- Rudolph, M.G., Bayer, P., Abo, A., Kuhlmann, J., Vetter, I.R., and Wittinghofer, A. (1998). The Cdc42/Rac interactive binding region motif of the Wiskott Aldrich syndrome protein (WASP) is necessary but not sufficient for tight binding to Cdc42 and structure formation. *J. Biol. Chem.* **273**, 18067–18076.
- Sanders, L.C., Matsumura, F., Bokoch, G.M., and de Lanerolle, P. (1999). Inhibition of myosin light chain kinase by p21-activated kinase. *Science* **283**, 2083–2085.
- Sells, M.A., and Chernoff, J. (1997). Emerging from the Pak: the p21-activated protein kinase family. *Trends Cell Biol.* **7**, 162–167.
- Sells, M.A., Boyd, J.T., and Chernoff, J. (1999). p21-activated kinase 1 (Pak1) regulates cell motility in mammalian fibroblasts. *J. Cell Biol.* **145**, 837–849.
- Smeal, T., Angel, P., Meek, J., and Karin, M. (1989). Different requirements for formation of Jun:Jun and Jun:Fos complexes. *Genes Dev.* **3**, 2091–2100.
- Thompson, G., Owen, D., Chalk, P.A., and Lowe, P.N. (1998). Deletion of the Cdc42/Rac-binding domain of p21-activated kinase. *Biochem. J.* **37**, 7885–7891.
- Tu, H., and Wigler, M. (1999). Genetic evidence for Pak1 autoinhibition and its release by Cdc42. *Mol. Cell Biol.* **19**, 602–611.
- Xu, W., Doshi, A., Lei, M., Eck, M.J., and Harrison, S.C. (1999). Crystal structures of c-Src reveal features of its autoinhibitory mechanism. *Mol. Cell* **3**, 629–638.
- Yablonski, D., Kane, L.P., Qian, D., and Weiss, A. (1998). A Nck-Pak1 signaling module is required for T-cell receptor-mediated activation of NFAT, but not of JNK. *EMBO J.* **17**, 5647–5657.
- Yang, W., and Cerione, R.A. (1997). Cloning and characterization of a novel Cdc42-associated tyrosine kinase, ACK-2, from bovine brain. *J. Biol. Chem.* **272**, 24819–24824.

Zenke, F.T., King, C.C., Bohl, B.P., and Bokoch, G.M. (1999). Identification of a central phosphorylation site in p21-activated kinase regulating autoinhibition and kinase activity. *J. Biol. Chem.* *274*, 32565–32573.

Zhang, S., Han, J., Sells, M.A., Chernoff, J., Knaus, U.G., Ulevitch, R.J., and Bokoch, G.M. (1995). Rho family GTPase regulate p38 mitogen-activated protein kinase through the downstream mediator Pak1. *J. Biol. Chem.* *270*, 23934–23936.

Zhao, Z.S., Manser, E., Chen, X.Q., Chong, C., Leung, T., and Lim, L. (1998). A conserved negative regulatory region in alphaPAK: inhibition of PAK kinases reveals their morphological roles downstream of Cdc42 and Rac1. *Mol. Cell. Biol.* *18*, 2153–2163.

#### Protein Data Bank ID Code

The coordinates reported in this paper have been deposited at the Protein Data Bank under ID code 1F3M.